Fiber-Embedded Electrolyte-Gated Field-Effect Transistors for e-Textiles

By *Mahiar Hamedi,* Lars Herlogsson, Xavier Crispin, Rebeca Marcilla, Magnus Berggren,* and *Olle Inganäs*

Electronic textiles (e-textile) are an emerging field[1] that can open new possibilities in a number of different areas. The concept of embedding a large number of components in fabrics is today subject of design analysis and simulation.[2,3] Some e-textile manufacturing schemes comprise the integration of conventional off-the-shelf electronic components by attaching these directly onto clothes. However, a key step for the integration of truly mass-produced e-textiles is to completely integrate electronic production with textile production. The integration of components directly onto the textile fibers requires functional materials and methods of using these. Conducting polymers are materials that fulfill the necessary requirements for e-textiles, and have previously been used for the construction of organic field-effect transistors (OFETs) directly on fibers.[4–6] These fiber OFETs are constructed on single fibers in four-layered structures, including an insulating dielectric material between channel and gate. Such structures, however, suffer from a number of drawbacks, including complexity of manufacturing, due to the necessity of adding four layers on the same fiber, very high operation voltages, and poor stability during mechanical stress on the fibers. We have previously demonstrated a way to circumvent some of these problems, by presenting an electrochemical transistor (ECT)[7] based on poly(3,4-ethylene dioxythiophene):poly(styrene sulfonate) (PEDOT:PSS) implemented directly on textile fibers.[8] These fiber ECTs present a number of advantages, such as high channel currents and ease of fabrication; a weakness is, however, the mode of operation, being restricted to only depletion mode, which complicates the design of logic circuits. Moreover, the electrochemical doping mechanism defining the principle of operation of this device, where the entire bulk of the channel has to be doped/undoped in order to switch the transistor, should put more limitations on the maximum switching speed. Another class of electrolyte-gated transistors comprises electric double-layer capacitor-gated OFETs (EDLC-OFETs). In contrast to ECTs, it is believed that only the conductivity of the semiconductor at its interface with the electrolyte is modulated by the electric field induced by the electrolyte polarization upon gate bias, leading to higher operation speeds. These types of transistors have been demonstrated on planar substrates that offer low driving voltages ($\leq$1 V), yielding high current densities and, recently, high switching speeds, surpassing 1 kHz in microdevices.[9–11]

Here, a fiber-based organic electrolyte-gated thin-film transistor (TFT) based on poly(3-hexylthiophene) (P3HT) and imidazolium ionic liquids is demonstrated. The demonstrated fiber TFTs are shown to operate in both field-effect and electrochemical operation modes, thus enabling both delivery of large currents or high speeds at low voltages. The transistors are further presented in a design scheme that is compatible with textile-production methods, thus enabling design of all woven logic and eventually all woven e-textiles. The design scheme involves the use of different functional fibers on reels, and weaving of these into fabrics to form electrical components whose functions depend on the structure and composition of the different fibers. This is taken into consideration in the method for creating bottom-contact organic TFTs (OTFTs) at fiber junctions, as seen in Figure 1a. Here, microgaps are created in a thin film of conducting material on top of fiber monofilaments. A semiconducting conjugated polymer is then coated to form a second layer. These functional fibers are weaved to create junctions with a second fully conducting fiber. The electrolyte-gated OTFTs are finally formed by depositing a solid-phase electrolyte at the fiber junctions (Fig. 1a).

The source-drain gaps, which have to be on the micrometer scale along the fiber, are created by weaving a fiber mesh, where the upper fibers are used as shadow masks for patterning the lower layer of fibers. A gold layer 100 nm thick is subsequently evaporated through these masks onto the lower fibers, creating a number of source and drain contacts, with a channel distance of 100 μm along each fiber, with the gap corresponding to the diameter of the shadow mask fibers. The fibers are then unweaved and rolled up for further use. The softness of gold and the good adhesion between gold and the fiber materials, such as nylon, result in coated fibers that tolerate the mechanical stresses induced by being rolled on reels and used in simple hand weaving. Next, thin films of purified regioregular P3HT are formed around the gold-coated fibers, by pulling these out of a solution (4 mg ml^{-1} in chloroform) at a relatively constant speed, to allow for the formation of continuous thin films (~100 nm) on

[*] Dr. M. Hamedi, Prof. O. Inganäs
Biomolecular and Organic Electronics
IFM, Center of Organic Electronics (COE)
Linköping University
581 83 Linköping (Sweden)
E-mail: mahiar@ifm.liu.se
Dr. L. Herlogsson, Prof. X. Crispin, Prof. M. Berggren
Organic Electronics, ITN
Linköping University
601 74 Norrköping (Sweden)
Dr. R. Marcilla
New Materials Department, CIDETEC
Center for Electrochemical Technologies
Paseo Miramo'n 196
Donostia-San Sebastia'n 20009, Gipuzkoa (Spain)

DOI: 10.1002/adma.200802681

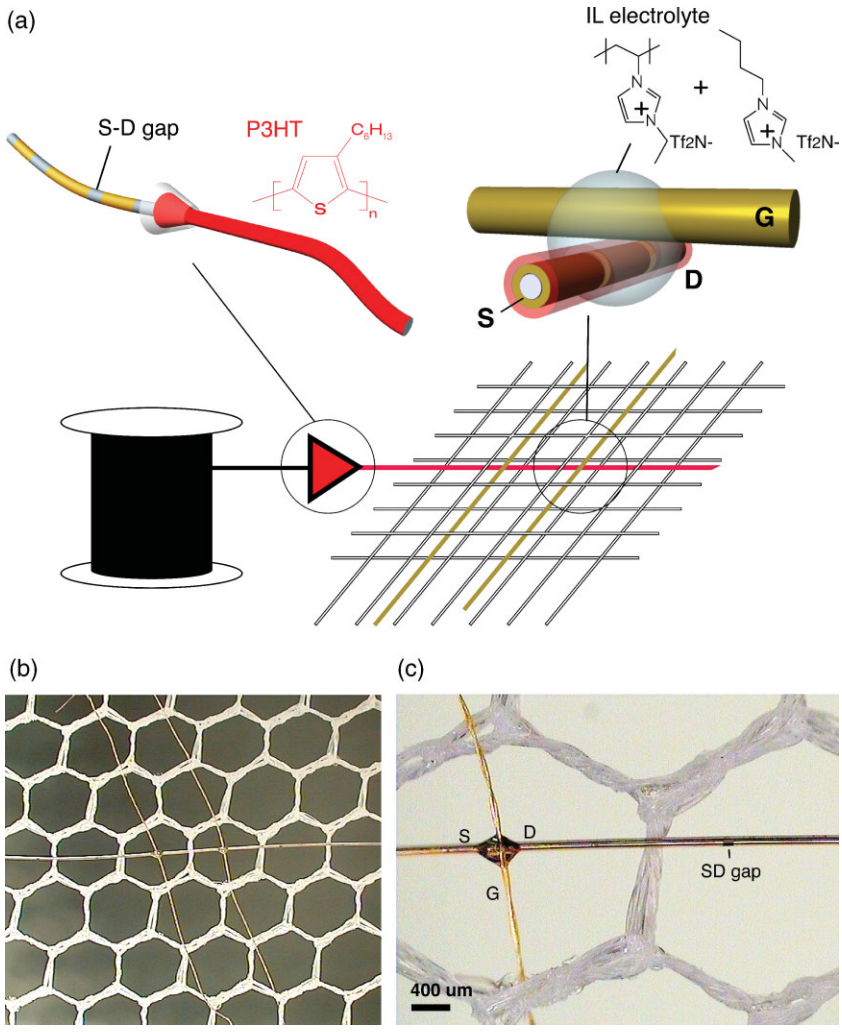

Figure 1. a) Schematics of: P3HT coating on top of fibers, with prepatterned source-drain gaps weaving of electrolyte-gated OTFT (top-left). Transistor formed at a fiber junction connected through an IL electrolyte (top-right) and weaving of transistors/devices using different fibers (bottom). b) Microscopy image of two transistors created along the horizontal fiber, all woven in a tulle. c) Microscopy image showing a close up of a fiber transistor on the left side, and a visible prepatterned transistor gap at the right side of the horizontal fiber.

the entire fiber. The transistors are then constructed using conventional textile production tools, where the P3HT-coated fibers are sewn inside textile tulle with a needle. Pure gold wires (bond-wires) are then sewn perpendicularly to the P3HT fibers to form junctions, each positioned above the microgaps, acting as gate contacts. Finally a drop of a solid polymeric ionic-liquid (IL) electrolyte is placed at the junctions, to create fiber OTFTs. Figure 1b shows two such transistors sewn along one wire, and Figure 1c shows a close up, with both the transistor and a gap visible. The solid IL electrolyte is a mixture of 1-butyl-3-methylimidazolium bis(trifluoromethanesulfonimide) ([bmim][Tf2N]) and a corresponding polymer IL poly(1-vinyl-3-methylimidazolium bis(trifluoromethanesulfonimide) (poly[ViEtIm][Tf2N], more information was published elsewhere[12]). The use of an electrolyte as gate insulator removes the necessity for a perfect alignment of the gate fiber electrode relative to the channel, and allows a wider range of distances between the gate and the channel, without altering significantly the electrical characteristics of the transistors.[9] Therefore, many functional fibers can be weaved with conventional textile-production techniques to form functional components at fiber junctions. This architecture allows for placing many transistors along a single fiber. Although gold is demonstrated here, it is believed that conducting polymers, such as polyaniline and PEDOT, can completely replace the gold in future developments.

The electrical characteristics of individual electrolyte-gated fiber OTFTs are measured under ambient conditions using a Keithley 4200 parameter-analyzer. Figure 2a shows electrical characteristics resembling those of a p-channel enhancement mode operation measured at $0.33\,V\ s^{-1}$. The fiber OTFT operates below $-1\,V$, and provides high saturation currents around $-30\,\mu A$ with current on/off ratios of $\sim$1000 at $V_{SD} = -1\,V$. 1 V. The effective capacitance of the transistor is measured using an HP 4192A impedance analyzer (the channel area is approximated from microscopy images). Figure 2d shows the evolution of the capacitance versus frequency reaching $C \approx 25\,\mu F\,cm^{-2}$ at low frequencies, in agreement with measurements on similar IL systems.[11,13] The I_G–V_G curve in Figure 2c is typical of a reversible capacitance charging/discharging, and hence, the capacitance can also be calculated using $I = C(dV/dt)$. Using $I = 8\ nA$, extracted from the half-width of the I_G–V_G curve, and a scan rate of $0.33\,V\,s^{-1}$, this capacitance value is similar (slightly higher) to the value obtained from the impedance spectroscopy at low frequencies.

The time response of the transistor, shown in Figure 3a, is recorded by applying a potential step to the gate from 0 V to -1 V. Here, a slow time response is measured with a parameter-analyzer, and the actual source current is presented. A faster time response is also recorded by measuring the voltage drop over a resistor put in series with the source electrode using an oscilloscope, and in the inset of Figure 3a the actual source channel current is presented, by subtracting the double-layer charging current from the measured source current (for more details see ref. [14]). The current peak at the beginning of the fast time response originates from the remaining stray capacitance (dis-)charging, which could not be subtracted with this method (note that this peak is not apparent in the slow time response, because it is averaged out by the parameter analyzer). As this remaining stray capacitive current vanishes after 3 ms, the current level reaches a quasi-plateau at $0.2\,\mu A$ (visible up to 10 ms), which is 100 times larger than the off-current ($V_G = 0\,V$, $t = 0$ s). This indicates that the channel opens in less than 3 ms

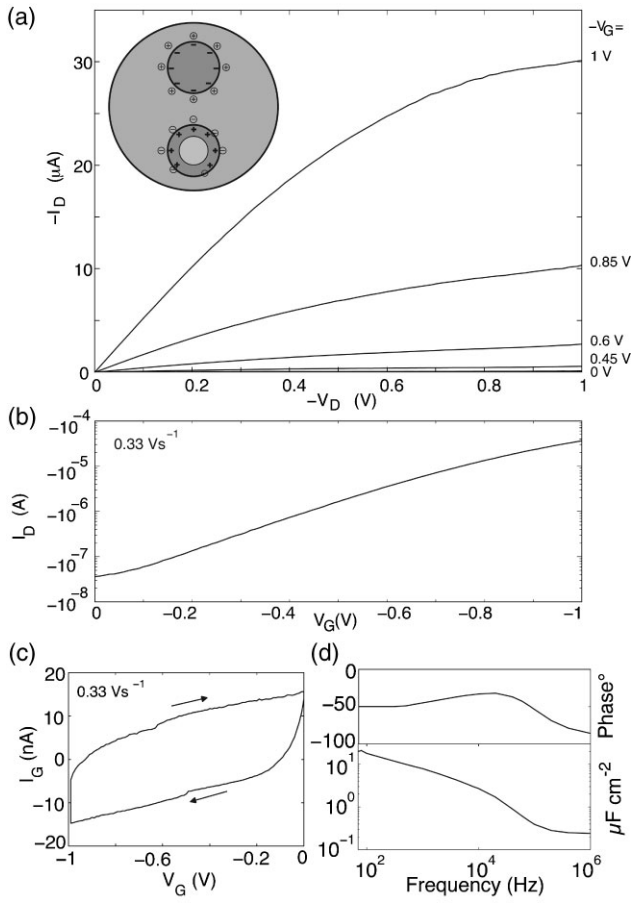

Figure 2. The electrical characteristics of a fiber EDLC-OTFT, similar to the one depicted in Figure 1c. a) Output characteristics. Inset: schematic of transistor operation with anions concentrated at the semi-conductor/electrolyte interface, and the cations located at the metal-gate/electrolyte interface. b) Transfer curves. c) I_G–V_G characteristics and d) effective transistor capacitance and corresponding phase-angle versus frequency.

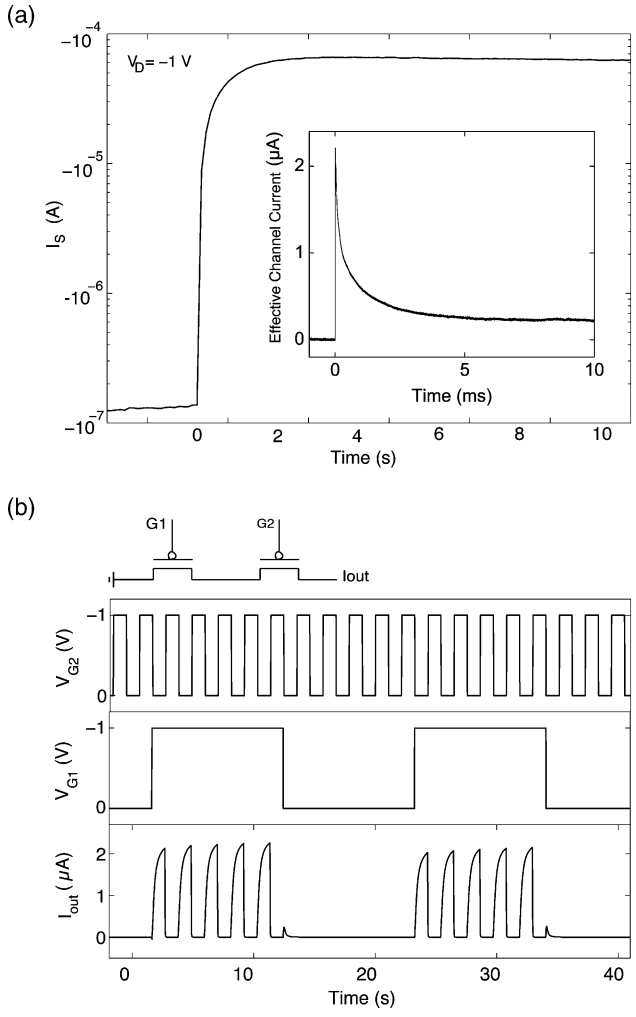

Figure 3. Transistor time response, measured by applying a potential step from 0 to −1 V. a) Source current response of the fiber transistor, at low time resolution. Inset: source current response obtained after subtracting the charging current at high time resolutions. b) Input voltages and output currents measured on a woven circuit based on two transistors, shown in Figure 1b. The model of the circuit is depicted on the top. The curves show a Boolean AND operation, with two inputs corresponding to gate voltages $V_{G1\text{-}2}$ and the output signal measured as output current I_{out}.

(∼330 Hz). However, the current level reached after this first plateau continues rising, slowly but significantly, up to 30 μA, and saturates after 2 s. These interesting results show that the channel of the fiber transistor opens in two regimes. i) The fast regime, which can be associated to a field-effect operation of the transistor as in the EDLC-OFETs.[9,10] The large current throughput of 0.2 μA in that regime is explained by the large capacitance of 5 μF cm^{-2} of an electric double-layer EDL, which is already partially formed in 3 ms, that is, at 330 Hz, as seen by impedance spectroscopy, in Figure 2d. ii) The second slow regime is associated to the bulk doping of the P3HT layer. After the EDL is rapidly formed at the P3HT-IL interface, some anions penetrate into the P3HT layer. In the channel, the positively doped P3HT chains (via hole injection from the source) are stabilized by mobile anions. Hence, the transistor starts to operate like an electrochemical (EC) transistor, and part of the P3HT layer is positively doped, until equilibrium is reached after 1–2 s, at the saturation current. By assuming a conductivity value of 10 S cm^{-1}, as measured experimentally for chemically doped P3HT,[15] and considering that bulk doping occurs throughout the circumference of the fiber, one can calculate a bulk doping depth to about 20 nm, at a saturated source-drain current of 30 μA.

Bulk doping can be further supported by the deviation of the phase angle of the impedance from −90° at low frequencies (Fig. 2d). A previously proposed model[16] of the kinetics of ion-intercalation electrodes, similar to the transistor channel here, suggest that ion trapping (i.e., trapping of the ionic-liquid anions in P3HT) leads to phase angles that lie in-between the Warburg diffusion limit (−45°) and the pure-capacitance limit (−90°), which is similar to what is observed here.

The demonstration of a dual operation mode resolved in time has not been reported previously (to the knowledge of the authors), and the success of these measurements might rely on

the combination of materials and geometries used here. It is noteworthy that the speed of the transistor is quite fast even in EC mode of operation, as a result of the high ion concentration and mobility of the IL electrolyte, and that the electrical characteristics of the EC mode are very similar to those in field-effect mode. These results show that more care should be taken in interpretation of the modes of operation[17] in electrolyte-gated transistors, as output curves that are usually measured in the Hertz regimes show very similar behavior to those in FETs.

The sketch in the inset of Figure 2a shows the distribution of anions and cations at the interfaces of the semiconductor and the gate electrode. The electric field caused by the applied gate voltage will be concentrated to the interfaces, meaning that the entire cylindrical transistor channel will be operational, even though the gate is placed on another fiber. This property is unique to the fiber-based electrolyte-gated devices, and cannot be achieved using conventional field-effect devices.

The surface roughness of the dip-coated P3HT film on microfibers is probably higher compared to spin-coated films on planar substrates. The operation of electrolyte-gated devices is, however, much more insensitive to surface roughness as compared to bottom-gated OFETs with pure dielectrics,[18] due to the formation of double-layers along the rough surface. Rougher surfaces could lead to increased bulk doping speeds.

The operation of the transistors is very stable over time, even in the electrochemical mode, and this is partially due to the use of the IL electrolyte.[11,19] Based on the stability, the good electrical characteristics of the fiber OTFTs, and the possibility of placing several transistors on a single fiber, a digital binary and operator containing two adjacent transistors on a single fiber is demonstrated in the electrochemical mode. The entire AND device is fully woven, as seen in Figure 1b. The curves in Figure 3b show the electrical in-/outputs of the device, clearly demonstrating high modulation switching of the out-current between on–off states, where a switching to the on-state only occurs when both gate voltages are on.

In summary, p-channel enhancement-mode electrolyte-gated OTFT transistors embedded on textile microfibers and digital devices based on these are demonstrated. The fiber transistor operates below 1 V, and delivers large current densities. The transience of the OFTF's current and the impedance spectroscopy measurements reveal that the channel is formed in two steps: first, a fast response attributed to a field-effect current modulation upon electric double-layer formation at the P3HT/electrolyte interface; second, a slow but major response associated to bulk electrochemical doping in the P3HT film.

In future development, functional microfibers, such as heterogeneous carbon-black[20] and carbon-nanotube fibers,[21] or conducting-polymer-based microfibers,[22–25] could allow replacement of the metallic gates and source-drains, since they can already deliver high enough currents. The only issue that has to be dealt with is designing these microfibers to be electrochemically stable under transistor-operation voltages. This would allow for mass-production of all polymer e-textiles, based on electrolyte-gated fiber components.

Furthermore, n-channel fiber transistors, already demonstrated for planar transistors,[26] could be formed in a similar method, in order to create complementary digital logics. The enhancement-mode fiber OTFT could be combined with depletion-mode fiber transistors[8] for advanced circuit designs. The fiber transistors can be improved by geometry and material optimization, in order to further reduce stray capacitances and allow for high speed (>kHz) large-area woven digital devices operating in the EDLC field-effect mode.

Acknowledgements

The Authors thank E. Said at ITN Linköping University for fruitful discussions, and D. Mecerreyes at CIDETEC for providing ionic liquids. This work is financed by the Center of Organic Electronics and funded by the Swedish Strategic Research Foundation SSF. Funding of equipment from the Knut and Alice Wallenberg foundation is gratefully acknowledged. R. M. acknowledges the Spanish Ministerio de Educación y Ciencia (MEC) for the funding of the project HOPE CSD2007-00007 (Consolider-Ingenio 2010).

Received: September 10, 2008
Revised: October 17, 2008
Published online: December 4, 2008

[1] R. F. Service, *Science* **2003**, *301*, 909.
[2] P. Stanley-Marbell, D. Marculescu, R. Marculescu, P. K. Khosla, *IEEE Trans. Comput.* **2003**, *52*, 996.
[3] J. C. Kao, R. Marculescu, *IEEE Trans. Comput.* **2006**, *55*, 745.
[4] J. B. Lee, V. Subramanian, *IEEE Trans. Electron Devices* **2005**, *52*, 269.
[5] M. Maccioni, E. Orgiu, P. Cosseddu, S. Locci, A. Bonfiglio, *Appl. Phys. Lett.* **2006**, 89.
[6] A. Bonfiglio, D. De Rossi, T. Kirstein, I. R. Locher, F. Mameli, R. Paradiso, G. Vozzi, *IEEE Trans. Inform. Technol. Biomed.* **2005**, *9*, 319.
[7] D. Nilsson, N. Robinson, M. Berggren, R. Forchheimer, *Adv. Mater.* **2005**, *17*, 353.
[8] M. Hamedi, R. Forchheimer, O. Inganäs, *Nat. Mater.* **2007**, *6*, 357.
[9] L. Herlogsson, X. Crispin, N. D. Robinson, M. Sandberg, O. J. Hagel, G. Gustafsson, M. Berggren, *Adv. Mater.* **2007**, *19*, 97.
[10] E. Said, X. Crispin, L. Herlogsson, S. Elhag, N. D. Robinson, M. Berggren, *Appl. Phys. Lett.* **2006**, 89.
[11] J. Lee, M. J. Panzer, Y. Y. He, T. P. Lodge, C. D. Frisbie, *J. Am. Chem. Soc.* **2007**, *129*, 4532.
[12] R. Marcilla, F. Alcaide, H. Sardon, J. A. Pomposo, C. Pozo-Gonzalo, D. Mecerreyes, *Electrochem. Commun.* **2006**, *8*, 482.
[13] V. Lockett, R. Sedev, J. Ralston, *J. Phys. Chem. C* **2008**, *112*, 7486.
[14] L. Herlogsson, Y.-Y. Noh, N. Zhao, X. Crispin, H. Sirringhaus, M. Berggren, *Adv. Mater.* **2008**, *20*, 1.
[15] X. Jiang, Y. Harima, K. Yamashita, Y. Tada, J. Ohshita, A. Kunai, *Chem. Phys. Lett.* **2002**, *364*, 616.
[16] J. Bisquert, *Electrochim. Acta* **2002**, *47*, 2435.
[17] M. J. Panzer, C. D. Frisbie, *J. Am. Chem. Soc.* **2007**, *129*, 6599.
[18] F. A. Yildirim, R. R. Schliewe, W. Bauhofer, R. M. Meixner, H. Goebel, W. Krautschneider, *Org. Electron. Phys. Mater. Applications* **2008**, *9*, 70.
[19] W. Lu, A. G. Fadeev, B. H. Qi, E. Smela, B. R. Mattes, J. Ding, G. M. Spinks, J. Mazurkiewicz, D. Z. Zhou, G. G. Wallace, D. R. MacFarlane, S. A. Forsyth, M. Forsyth, *Science* **2002**, *297*, 983.
[20] J. Sanchez-Gonzalez, A. Macìas-Garcìa, M. F. Alexandre-Franco, V. Gomez-Serrano, *Carbon* **2005**, *43*, 741.
[21] I. Alig, D. Lellinger, M. Engel, T. Skipa, P. Potschke, *Polymer* **2008**, *49*, 1902.

[22] C. Muller, S. Goffri, D. W. Breiby, J. W. Andreasen, H. D. Chanzy, R. A. J. Janssen, M. M. Nielsen, C. P. Radano, H. Sirringhaus, P. Smith, N. Stingelin-Stutzmann, *Adv. Funct. Mater.* **2007**, *17*, 2674.
[23] J. Foroughi, G. M. Spinks, G. G. Wallace, P. G. Whitten, *Synth. Met.* **2008**, *158*, 104.
[24] A. Mirmohseni, D. Salari, R. Nabavi, *Iran. Polym. J.* **2006**, *15*, 259.
[25] S. J. Pomfret, P. N. Adams, N. P. Comfort, A. P. Monkman, *Polymer* **2000**, *41*, 2265.
[26] M. J. Panzer, C. D. Frisbie, *J. Am. Chem. Soc.* **2005**, *127*, 6960.